Earth Syst. Sci. Data, 4, 167–186, 2012
www.earth-syst-sci-data.net/4/167/2012/
doi:10.5194/essd-4-167-2012

Open Access Earth System Science Data

The global distribution of pteropods and their contribution to carbonate and carbon biomass in the modern ocean

N. Bednaršek[1], J. Možina[2], M. Vogt[3], C. O'Brien[3], and G. A. Tarling[4]

[1]NOAA Pacific Marine Environmental Laboratory, 7600 Sand Point Way NE, Seattle, WA 98115, USA
[2]University of Nova Gorica, Laboratory for Environmental Research, Vipavska 13, Rožna Dolina, 5000 Nova Gorica, Slovenia
[3]Institute for Biogeochemistry and Pollutant Dynamics, ETH Zürich, Universitaetstrasse 16, 8092 Zürich, Switzerland
[4]British Antarctic Survey, Natural Environment Research Council, High Cross, Madingley Road, Cambridge CB3 0ET, UK

Correspondence to: N. Bednaršek (nina.bednarsek@noaa.gov)

Received: 20 March 2012 – Published in Earth Syst. Sci. Data Discuss.: 10 May 2012
Revised: 8 October 2012 – Accepted: 19 October 2012 – Published: 10 December 2012

Abstract. Pteropods are a group of holoplanktonic gastropods for which global biomass distribution patterns remain poorly described. The aim of this study was to collect and synthesise existing pteropod (Gymnosomata, Thecosomata and Pseudothecosomata) abundance and biomass data, in order to evaluate the global distribution of pteropod carbon biomass, with a particular emphasis on temporal and spatial patterns. We collected 25 939 data points from several online databases and 41 scientific articles. These data points corresponded to observations from 15 134 stations, where 93 % of observations were of shelled pteropods (Thecosomata) and 7 % of non-shelled pteropods (Gymnosomata). The biomass data has been gridded onto a $360 \times 180^{\circ}$ grid, with a vertical resolution of 33 depth levels. Both the raw data file and the gridded data in NetCDF format can be downloaded from PANGAEA, doi:10.1594/PANGAEA.777387. Data were collected between 1950–2010, with sampling depths ranging from 0–2000 m. Pteropod biomass data was either extracted directly or derived through converting abundance to biomass with pteropod-specific length to carbon biomass conversion algorithms. In the Northern Hemisphere (NH), the data were distributed quite evenly throughout the year, whereas sampling in the Southern Hemisphere (SH) was biased towards winter and summer values. 86 % of all biomass values were located in the NH, most (37 %) within the latitudinal band of 30–60° N. The range of global biomass values spanned over four orders of magnitude, with mean and median (non-zero) biomass values of 4.6 mg C m^{-3} (SD = 62.5) and 0.015 mg C m^{-3}, respectively. The highest mean biomass was located in the SH within the 70–80° S latitudinal band (39.71 mg C m^{-3}, SD = 93.00), while the highest median biomass was in the NH, between 40–50° S (0.06 mg C m^{-3}, SD = 79.94). Shelled pteropods constituted a mean global carbonate biomass of 23.17 mg $CaCO_3$ m^{-3} (based on non-zero records). Total biomass values were lowest in the equatorial regions and equally high at both poles. Pteropods were found at least to depths of 1000 m, with the highest biomass values located in the surface layer (0–10 m) and gradually decreasing with depth, with values in excess of 100 mg C m^{-3} only found above 200 m depth.

Tropical species tended to concentrate at greater depths than temperate or high-latitude species. Global biomass levels in the NH were relatively invariant over the seasonal cycle, but more seasonally variable in the SH. The collected database provides a valuable tool for modellers for the study of marine ecosystem processes and global biogeochemical cycles. By extrapolating regional biomass to a global scale, we established global pteropod biomass to add up to 500 Tg C.

Published by Copernicus Publications.

1 Introduction

The phylum Mollusca comprises at least 100 000 species, of which only 4000 species inhabit the upper ocean, principally those in the class Gastropoda. Approximately 140 species are holoplanktonic, meaning that they do not inhabit the seabed during any stage of their life cycle. The holoplanktonic lifestyle is facilitated by adaptations such as the development of swimming appendages and the reduction or loss of the calcareous shell. The pteropods are holoplanktonic gastropods that are widespread and abundant in the global ocean (Lalli and Gilmer, 1989). They consist of two orders: the Thecosomata (shelled pteropods) and the Gymnosomata (naked pteropods). The two orders are taxonomically separated not only by their morphology and behaviour, but also by their trophic position within the marine food web, with the former consisting mainly of herbivores and detritivores (Hopkins, 1987; Harbison and Gilmer, 1992) and the latter of carnivores (Lalli, 1970). A further systematic detail divides order Thecosomata into two suborders, the Euthecosomes and Pseudothecosomes. The two suborders have similar lifestyles, but they are set apart by their anatomical characteristics, most notably a gelatinous internal pseudoconch in Pseudothecosomes that replaces the external shell present in Euthecosomes (Lalli and Gilmer, 1989).

Pteropods have high ingestion rates that are in the upper range for mesozooplankton (Perissinotto, 1992; Pakhomov and Perissinotto, 1997). Although pteropods constitute, on average, only 6.5 % of the total abundance density of grazers in areas such as the Southern Ocean, they contribute on average 25 % to total phytoplankton grazing and consume up to 19 % of daily primary production (Hunt et al., 2008). Pteropods themselves are also an important prey item for many predators, such as larger zooplankton as well as herring, salmon and birds (Hunt et al., 2008; Karnovsky et al., 2008).

Pteropods are also involved in numerous pathways of organic carbon export. They contribute to the downward flux of carbon through the production of negatively buoyant faecal pellets. A number of pteropods also produce pseudo-faeces, i.e. accumulations of rejected particles expelled in mucous strings (Gilmer, 1990). Pteropods feed using mucous webs that trap fine particles and small faecal pellets, which form fast sinking colloids when abandoned (Jackson et al., 1993; Gilmer and Harbison, 1991). Pteropods actively transport carbon downwards during the descent phase of nycthemeral migrations, mostly from the shallow euphotic zone into the deeper twilight zone, where they respire and defecate.

In terms of inorganic carbon, pteropods are one of only a few taxa that make their shells out of aragonite as opposed to the calcite form of calcium carbonate. The biogeochemical importance of aragonite production by pteropods has been shown in a number of studies (Berner and Honjo, 1981; Acker and Byrne, 1989). Their aragonite shell not only contributes to the transfer of inorganic material into the deep ocean (Tréguer et al., 2003) but also increases the weight of pteropods as settling particles and hence their sinking speed (Lochte and Pfannkuche, 2003). Ontogenetic (or seasonal) migration, often followed by mass mortality, transports both organic and inorganic carbon to depth (Tréguer et al., 2003). On a global scale, aragonite production by pteropods might constitute at least 12 % of the total carbonate flux worldwide (Berner and Honjo, 1981).

Although the ecological and biogeochemical importance of pteropods has been well recognised, essential details on their global biomass distribution remain poorly resolved. Such information is required for modellers to be able to incorporate this group as a plankton functional type within ecosystem models and to allow the quantification of their contribution to carbon export in biogeochemical models.

The Marine Ecosystem Model Inter-comparison Project (MAREMIP) has been launched as an initiative to compare current plankton functional type models, and to collect data necessary for their validation. In 2009, MAREMIP launched the MARine Ecosystem DATa project, with the aim to construct a database based on field measurements for the biomass of ten major plankton functional types (PTFs) currently represented in marine ecosystem models (Le Quéré et al., 2005). The resulting biomass databases include diatoms (silicifiers), *Phaeocystis* (DMS producers), coccolithophores (calcifying phytoplankton), diazotrophs (nitrogen fixers), picophytoplankton, bacterioplankton, mesozooplankton, macrozooplankton and pteropods and foraminifera (calcifying zooplankton). All MAREDAT data sets of global biomass distribution are publicly available and will serve marine ecosystem modellers for model evaluation, development and future model inter-comparison studies. This study will present and evaluate the seasonal and temporal distribution of pteropod carbon biomass, with a particular emphasis on the seasonal and vertical biomass patterns. Finally, global estimates of pteropod biomass and productivity will be presented.

2 Data

2.1 Origin of data

The sources of the data were several online databases (PANGEA, ZooDB, NMFS127 COPEPOD) and 41 scientific articles. The full data set is comprised of 25 939 data points (Table 1). Each data point includes the following information: Year, Month, Day, Longitude, Latitude, Sampling Depth (m), Mesh size (μm) Abundance (ind. m^{-3}) and Biomass (mg C m^{-3}) and the data source. All data points presenting abundance measurements were later converted to biomass values. Zero biomass values were included as biologically valid data points in the data set. Some data sets included multiple samples at several stations, which would bias the global biomass estimates if not suitably treated. Thus, when repeat sampling of the same station location

Table 1. The list of data contributors in alphabetical order, with the two major online databases listed at the end of the list.

Entry No.	Principal Investigator	Database	Year (data collection)	Region
1	Andersen et al. (1997)	PANGEA	1991–1992	NE tropical Atlantic
2	Bednaršek et al. (2012)	–	1996–2010	Southern Ocean (Scotia Sea)
3	Bernard and Froneman (2005)	–	2004	Southern Ocean (west-Indian sector of the Polar Frontal Zone)
4	Bernard and Froneman (2009)		2002/2004/2005	Indian sector PFZ
5	Blachowiak-Samolyk et al. (2008)	–	2003	Arctic (N Svalbard waters)
6	Boysen-Ennen et al. (1991)	–	1983	Antarctica (Weddell Sea)
7	Broughton and Lough (2006)	–	1997	North Atlantic (Georges Bank)
8	Clarke and Roff (1990)	–	1986	Caribbean Sea (Lime Cay)
9	Daase and Eiane (2007)	–	2002–2004	Arctic (N Svalbard waters)
10	Dvoretsky and Dvoretsky (2009)	–	2006	E Barents Sea (Novaya Zemlya)
11	Elliot et al. (2009)	–	2006–2007	Antarctica (McMurdo Sound)
12	Flores et al. (2011)	–	2004–2008	Southern Ocean (Lazarev Sea)
13	Foster (1987)	–	1985	Antarctica (McMurdo Sound)
14	Froneman et al. (2000)	–	1998	Southern Ocean (Prince Edward Archipelago)
15	Hunt and Hosie (2006)	–	2001–2002	Southern Ocean (south of Australia)
16	Koppelmann et al. (2004)	PANGEA	1999	Eastern Mediterranean Sea
17	Marrari et al. (2011)	–	2001/2002	W Antarctic (Marguerite Bay)
18	Mazzocchi et al. (1997)	PANGEA	1991–2002	Eastern Mediterranean Sea
19	Mileikovsky (1970)	–	1966	North Atlantic, Subarctic and North Pacific Ocean
20	Moraitou-Apostolopoulou et al. (2008)	PANGEA	1994	Eastern Mediterranean Sea
21	Mousseau et al. (1998)	–	1991–1992	NW Atlantic (Scotian Shelf)
22	Nishikawa et al. (2007)	–	2000–2002	Pacific Ocean (Sulu Sea, Celebes Sea, South China Sea)
23	Pakhomov and Perissinotto (1997)	–	1993	Southern Ocean (Subtropical Convergence)
24	Pane et al. (2004)	–	1995	Antarctica (Ross Sea)
25	Fernandez de Puelles et al. (2007)	–	1994–2003	Western Mediterranean
26	Ramfos et al. (2008)	PANGEA	2000	Eastern Mediterranean
27	Rogachev et al. (2008)	–	2004	W Pacific Ocean (Academy Bay, Sea of Okhotsk)
28	Schalk (1990)	–	1984–1999	Indo-Pacific waters (E Banda Sea, W Arafura Sea)
29	Schiebel et al. (2002)		1997/1999	S of Azores Islands
30	Schnack-Schiel and Cornils (2009)	PANGEA	2005	Pacific Ocean (Java Sea)
31	Siokou-Frangou et al. (2008)	PANGEA	1987–1997	Eastern Mediterranean
32	Solis and von Westernhagen (1978)	–	1972	Philippines (Hilutangan Channel)
33	Swadling et al. (2011)	–	2004–2008	E Antarctica (Dumont d'Urville Sea)
34	Volkov (2008)	–	1984–2006	Okhotsk Sea, Bering Sea, NWP
35	Ward et al. (2007)	–	2004–2005	Southern Ocean (S&W of Georgia)
36	Wells Jr. (1973)	–	1972	N Atlantic Ocean (Barbados)
37	Werner (2005)	–	2003	Arctic (W Barents Sea)
38	Wormuth (1985)	–	1975–1977	N Atlantic Ocean (NW Sargasso Sea)
39	Zervoudaki et al. (2008)	PANGEA	1997–2000	Eastern Mediterranean
40	NMFS-COPEPOD (2011) NOAA (National Oceanic and Atmospheric Administration)	COPEPOD – The global plankton database	1953–2001	Global data set
41	ZooDB (2011), Ohman	ZooDB – Zooplankton database	1951–1999	Pacific Ocean (Southern and Central California)

was conducted in a single day (for instance through sampling both night and day or with different mesh-sized nets), a mean biomass at that station was calculated and used in subsequent processing. As the sampling methodology can introduce major errors in the biomass estimates, a systematic characterisation of the sampling gear, was also included to allow sources of error to be identified. In addition, all details on pteropod species composition and life stages were

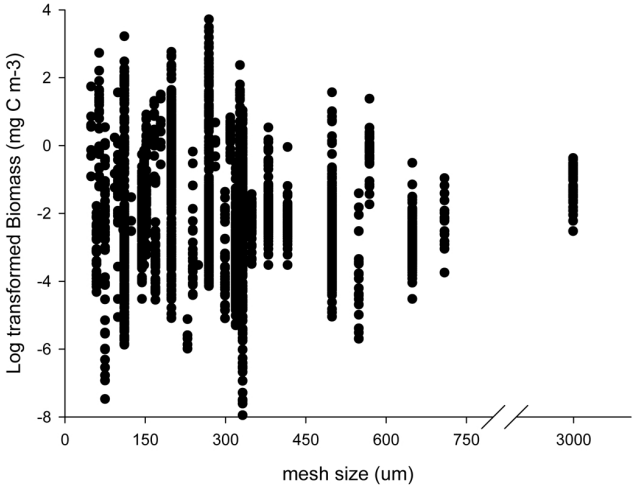

Figure 1. The relationship between net mesh size and pteropod biomass.

documented within the database. Where there were a number of species identified per station, we also provided summary statistics of total pteropod biomass per station (n = 14 136). The database included both Gymnosomata and Thecosomata, encompassing all genera included in the taxonomic tree, which was taken from Marine Species Identification Portal (http://species-identification.org) presented in Fig. 3. Further subspecies levels (or formae) were not resolved within the database. No observations of the suborder Pseudothecosomata were reported in the source data sets.

2.2 Quality control

The identification and rejection of statistical outliers in the summarised biomass data set was performed using Chauvenet's criterion (Glover et al., 2011; Buitenhuis et al., 2012). Based on this statistical analysis, none of the stations were excluded as outliers (two sided z-score = 4.1257).

2.3 Methodology for biomass conversion

Of the data sets obtained, the majority only reported values for abundance (ind. m^{-3}), with very few providing biomass values (mg m^{-3}). Furthermore, abundance data was collected with varying mesh sizes and net-sampling strategies, which might introduce uncertainties. Therefore, we have reported the mesh sizes and net sampling strategy in the database whenever this information was available (PANGEA Table). In certain cases, multiple mesh-sized samplers were used, of which we have included all descriptions available. No data were excluded on the basis of mesh size and we examine the influence of mesh size in the Results section (Figs. 1 and 2).

Where direct biomass values were not available, we calculated biomass as a product of abundance and dry weight (DW, mg). To estimate DW, the length (L, mm) of organisms

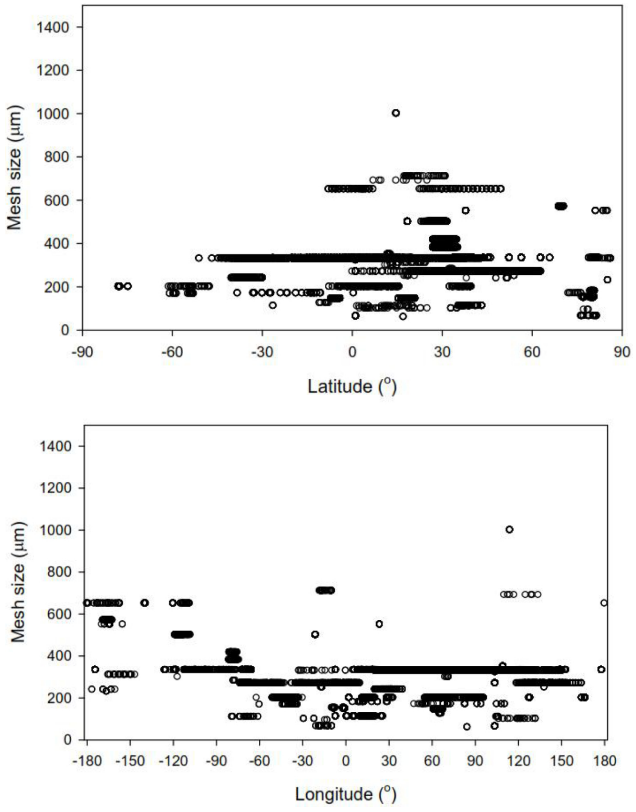

Figure 2. Net-mesh size versus longitude (above) and latitude (below). Data was excluded if multiple mesh sizes were reported.

was first converted to wet weight (WW, mg) using various conversions (see below), with subsequent conversion to dry weight (Table 2).

For many pteropod species, specific length-to-wet weight conversions were not available so more general length-weight conversions for pteropods were applied based on those used by the GLOBal ocean ECosystems dynamics (GLOBEC) data management program. In GLOBEC, wet weights (WW) of different pteropod families were calculated based on their specific body geometry and length (Little and Copley, 2003). The GLOBEC conversions covered the barrel shaped *Clione* family of naked pteropods, the cone shaped family of *Styliola*, the low-spire (globular) family of *Limacina* spp., and the pyramidally shaped family of *Clio* spp. Accordingly, we assorted groups or species into respective geometric shapes and then applied the GLOBEC L to WW conversions. Although species-specific conversions are lacking for many of the groups (Table 2), we believe that this approach provides a reasonable first order approximation of individual biomass for the purpose of the present analysis. More specific details of these conversions are given below:

Equation (1) was used to convert all non-shelled (naked) taxa, including barrel-and oval- shaped families of *Spongiobranchia* spp., *Pneumodermopsis* and *Paedoclione* and class Gymnosomata (Little and Copley, 2003). Equation (2) was

Table 2. Length to weight equations for different pteropod groups based on the geometric shapes.

SPECIES	Group	Equation source	Conversion	Equation name	Equation (size-weight relationship)	Equation (Davis and Wiebe, 1985)	
Limacina helicina	Round/cylindrical/globular	Bednaršek et al. (2012)	Diameter→DW		$DW = 0.137 \times D^{1.5005}$		
Limacina spp.	Round/cylindrical/globular	GLOBEC	Diameter→DW		$WW = 0.000194 \times L^{2.5473}$	WW→DW	WW×0.28
Clione spp.	Barell/oval-shaped (naked)	GLOBEC	Length→WW	Pteropod (naked: Clione)	$WW = 10^{(2.533 \times \log(L) - 3.89095) \times 10^3}$	WW→DW	WW×0.28
Hyalocylis spp.	Cone/needle/tube/bottle-shaped	GLOBEC	Length→WW	Pteropod (cone-shaped: Styliola)	$WW = PI \times L^{3 \times 3/25}$	WW→DW	WW×0.28
Styliola spp.	Cone/needle/tube/bottle-shaped	GLOBEC	Length→WW	Pteropod (cone-shaped: Styliola)	$WW = PI \times L^{3 \times 3/25}$	WW→DW	WW×0.28
Spongiobranchaea spp.	Barell/oval-shaped (naked)	GLOBEC	Length→WW	Pteropod (naked: Clione)	$WW = 10^{(2.533 \times \log(L) - 3.89095) \times 10^3}$	WW→DW	WW×0.28
Pneumodermopsis and *Paedoclione*	Barell/oval-shaped (naked)	GLOBEC	Length→WW	Pteropod (naked: Clione)	$WW = 10^{(2.533 \times \log(L) - 3.89095) \times 10^3}$	WW→DW	WW×0.28
Cavolinia spp.	Triangular/pyramidal	GLOBEC	Length→DW	Pteropod (Clio)	$WW = 0.2152 \times L^{2.293}$	WW→DW	WW×0.28
Clio spp.	Triangular/pyramidal	GLOBEC	Length→WW	Pteropod (Clio)	$WW = 0.2152 \times L^{2.293}$	WW→DW	WW×0.28
Creseis spp.	Cone/needle/tube/bottle-shaped	GLOBEC	Length→WW	Pteropod (cone-shaped: Styliola)	$WW = PI \times L^{3 \times 3/25}$	WW→DW	WW×0.28
Cuvierina spp.	Cone/needle/tube/bottle-shaped	GLOBEC	Length→WW	Pteropod (cone-shaped: Styliola)	$WW = PI \times L^{3 \times 3/25}$	WW→DW	WW×0.28
Diacria spp.	Triangular/pyramidal	GLOBEC	Length→WW	Pteropod (Clio)	$WW = 0.2152 \times L^{2.293}$	WW→DW	WW×0.28
Thecosomata	Shelled	Davis and Wiebe (1985)	Length→WW		$WW = 0.2152 \times L^{2.293}$	WW→DW	WW×0.28
Gymnosomata	Naked	Davis and Wiebe (1985)	Length→WW		$WW = 10^{(2.533 \times \log(L) - 3.89095) \times 10^3}$	WW→DW	WW×0.28
Pteropoda	Shelled	Davis and Wiebe (1985)	Length→WW		$WW = 0.2152 \times L^{2.293}$	WW→DW	WW×0.28

applied to *Clione* spp., being a genus species conversion equation originally derived by Böer et al. (2005):

$$WW = 10^{(2.533 \times \log(L) - 3.89095) \times 10^3}, \quad (1)$$

$$DW = 1.6146^{e0.0088 \times L}. \quad (2)$$

Three different shapes were distinguished within the shelled taxa, each with their own L to WW conversions:

$$WW = WW = 0.2152 \times L^{2.293} \text{ triangular/pyramidal shaped (Davis and Wiebe, 1985)} \quad (3)$$

$$WW = 0.000194 \times L^{2.5473} \text{ round/cylindrical/globular shaped (Little and Copley, 2003)} \quad (4)$$

$$WW = PI \times L^{3 \times 3/25} \text{ cone/needle/bottle-shaped (Little and Copley, 2003).} \quad (5)$$

Limacinidae were one of the most abundant taxa within our database, for which there are several published L to DW conversions in the literature:

$$DW = 0.257L^{2.141} \text{ (Gannefors et al., 2005)} \quad (6)$$

$$\log DW = 0.685L^{-2.222} \text{ (Fabry, 1989)} \quad (7)$$

$$DW = 0.1365L^{1.501} \text{ (Bednaršek et al., 2012).} \quad (8)$$

Gannefors et al. (2005), Fabry (1989) and Bednaršek et al. (2012) fitted the respective functions to differing size ranges of *Limacinidae*, so we compared their performance across a uniform size range to consider their suitability for more broad scale application (Appendix B, Fig. B1). The functional form of Fabry (1989), although optimal for animals in a size range between 1 and 4 mm, became exponentially large at shell diameters above this range so was considered unsuitable for the present analysis. The Gannefors et

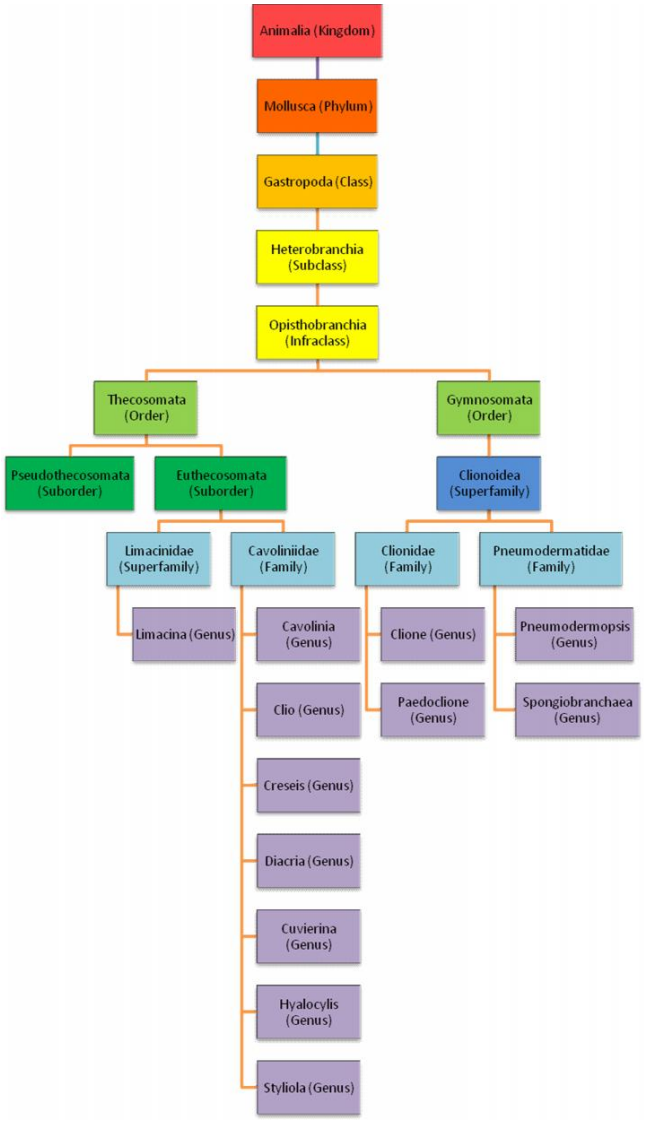

Figure 3. Taxonomy of pteropods.

al. (2005) and Bednaršek et al. (2012) functional forms performed similarly well and realistically (Appendix B) across the shell diameter size ranges encountered in the present study (0.01 to 50 mm). We chose the Bednaršek et al. (2012) function given that its estimate of dry weight between 1 and 4 mm shell diameter fell midway between the estimates of the Fabry (1989) and Gannefors et al. (2005) algorithms, combined with the fact that its behaviour remained realistic at larger size categories.

In cases, where the data-source referred to orders or classes rather than species, Eq. (3) was applied since the taxa were principally non-*Limacinidae* shelled species.

In the case of juveniles, the above length to weight conversions were used according to their respective taxa or body shape, but the length of the veligers and larvae set at 10 % of the adult average size, which is based on our own comparisons of average juvenile and adult sizes.

2.3.1 Calculation of length for the individual pteropod species

For some data records, only the species and abundance was recorded without any indication of individual size or weight. Individual shell diameter was therefore inferred in order to calculate biomass. Our first step was to determine size of adult specimens of each species using information from the Marine Species Identification Portal (http://species-identification.org/), of which results are presented in Appendix C (Table C1), along with the body shape, length and mean size.

Where the abundance data was given for a higher taxonomic level than species (e.g. class, suborder, order), the average length across all species within that respective taxa was determined (Table C1). Because this procedure only took account of adult sizes, we were aware that this would result in an overestimation of biomass. This was compensated for in two ways: firstly, by taking into account data points where a juvenile status was indicated (283 in total, representing 2 % of entire database) in which case length was assumed to be 10 % of adult size (see above). Secondly, where the data was not species-specific (but family- or higher order-specific), the average length across all species within the taxon was calculated, so preventing extreme bias from very large or very small species.

Unfortunately, the lack of data points where both biomass and abundance values were reported made it impossible to do a quantitative comparison of the performance of our L to W conversions.

2.3.2 Calculation of dry weight and carbon biomass from wet weight

Wet weight was converted to dry weight using Davis and Wiebe (1985):

$$DW = WW \times 0.28. \quad (9)$$

Biomass was subsequently transformed to carbon using a conversion factor of 0.25, following Larson (1986).

2.3.3 Global contribution of shelled pteropods to carbonate biomass

Once conversions from abundance to carbon biomass had been completed, we considered the global biomass distribution of both shelled and non-shelled pteropod taxa. Separating out the shelled pteropod taxa allows the global carbonate distribution resulting from pteropods to be assessed, so permitting the evaluation of their contribution to the global carbonate budget. Bednaršek et al. (2012) have calculated inorganic carbon as a percentage of total organic subtracted from total carbon, deducing the PIC/POC ratio of 0.27 vs. 0.73.

Table 3. Mean, median, maximum and minimum and standard deviation (SD) of pteropod biomass (mg C m^{-3}) determined (i) for all global data, (ii) all non-zero data points, (iii) all non-zero Northern Hemisphere (NH) data-points and (iv) all non-zero Southern Hemisphere (SH) data-points.

summed biomass data	mean	median	max	min	SD
all global data	4.09	0.008	5.05e+003	0.00	59.06
non-zero global data	4.58	0.0145	5.05e+003	1.00e-006	62.46
for the NH non-zero data	4.04	0.0145	5.05e+003	1.00e-006	64.84
for the SH non-zero data	8.15	0.001	608.35	2.00e-006	45.36

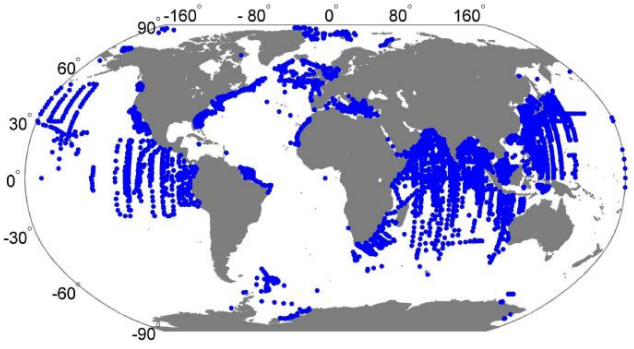

Figure 4. Global distribution of quality-controlled pteropod data.

Assuming that all inorganic carbon is in the form of calcium carbonate, the amount of calcium carbonate can be estimated as follows:

$$CaCO_3\ (\%) = [TC\ (\%) - TOC\ (\%)] \times 8.33 \quad (10)$$

where the constant 8.33 represents the molecular mass ratio of carbon to calcium carbonate.

3 Results

3.1 Global data distribution of biomass data

Altogether, we collected 25 939 data entries across all oceanic regions, which corresponded to 15 134 samples of total pteropod biomass (Fig. 4). Out of these, 14 136 data points (93 %) represented shelled pteropods (Thecosomes), and the remaining 7 % represented non-shelled pteropods (Gymnosomes). Within the whole data set, 1608 data points (11 % of all values) were reported as zero values for all pteropod groups.

Although pteropod observations were available for all ocean basins, there was a clear bias of the data towards observations in the Northern Hemisphere (NH) (77 % of non-zero entries), with the remaining 23 % in the Southern Hemisphere (SH, Table 3 and 6, Fig. 4). With respect to latitude, the most entries (37 %) were collected within the latitudinal band of 10–60° N (Table 4).

The maximum net sampling depth was 2000 m but 83 % of all nets were sampled to a maximum depth of 200 m (Table 5). Across all observations, 62 % of all biomass occurred within the top 200 m, with the remaining biomass (38 %) being relatively evenly distributed down to 2000 m. The deepest occurrence of pteropods in our database was 2000 m, located at 81° N,163° E. The highest biomass for shelled pteropods (2980 mg C m^{-3}) was recorded at the surface in the NH temperate region, at 42° N,70° W. The highest biomass for the non-shelled pteropods (5045 mg C m^{-3}) was recorded in the same region (42° N,66° W). There were very few direct measurements of pteropod biomass (see Sect. 2.3), but of those, the highest recorded values were in the Sea of Okhotsk (54° N,138° E), where biomass reached 538 mg C m^{-3} (Rogachev et al., 2008).

3.2 The effect of nets and mesh sizes on global pteropod biomass

Mesh size will influence the size range of organisms captured by nets. In assembling this database, we decided to include all net-catch data, irrespective of mesh size. This will undoubtedly create error, particularly in the undersampling of smaller individuals by larger meshed nets through the lack of retention and of larger, more motile individuals by finer meshed nets through avoidance. For the purpose of the present analysis, with a focus mainly on comparative patterns, it is important that these errors do not generate bias, since this could distort any discerned geographic trends. We considered this in two ways. In Fig. 1, we compared the biomass to net mesh size across 19 671 samples. The figure shows a peak in biomass towards the mid-size meshes (~ 300 μm). This demonstrates that the majority of biomass lay within organisms with an equivalent spherical diameter of 300 μm or greater, and that the undersampling of smaller organisms by some studies is unlikely to have a considerable impact on biomass estimates. Equally, the figure is indicating that the average biomass is similar, regardless of the mesh size used for sampling.

In Fig. 2, net mesh-size was compared to latitude. Although this illustrates the considerable variety of meshes used within the present database, it also shows there was no apparent bias towards certain mesh size being used at some latitudes more than others. Therefore, although the use of different meshes between studies is undoubtedly a source of

Table 4. Latitudinal distribution of abundance data in ten degree latitudinal bands (90° to 90°). Mean, maximum (max), median and standard deviation (SD) of biomass (mg C m^{-3}) per latitudinal band, calculated from non-zero data points.

Latitude	Entries	Mean (mg C m^{-3})	SD	Max (mg C m^{-3})	Min (mg C m^{-3})	Median (mg C m^{-3})
90 to 80° S	0	–	–	–	–	–
80 to 70° S	72	27.20	98.44	557.41	0.001	0.19
70 to 60° S	59	0.09	0.42	2.63	2.00e-006	0
60 to 50° S	90	13.93	35.55	168.47	0.01	0.48
50 to 40° S	90	0.25	2.27	21.53	8.00e-006	1.32e-004
40 to 30° S	127	0.02	0.07	0.64	2.83e-006	8.80-005
30 to 20° S	167	0.01	0.05	0.45	5.33e-006	2.18e-004
20 to 10° S	310	0.02	0.08	0.86	3.25e-006	6.14e-004
10° N to 0°	1007	11.93	53.98	608.35	3.50e-006	0
0° to 10° N	1078	0.06	0.26	4.30	4.67e-006	0.01
10° to 20° N	2044	1.47	8.91	226.66	1.00e-006	0.01
20° to 30° N	1725	0.06	0.49	9.85	8.00e-006	0.003
30° to 40° N	2958	4.51	21.65	362.89	1.00e-006	0.01
40° to 50° N	744	34.76	248.13	5.05e+003	2.90e-005	0.09
50° to 60° N	1960	1.26	17.26	538	0.003	0.40
60° to 70° N	896	0.31	0.46	11.82	0.003	026
70° to 80° N	77	17.31	61.97	517.05	1.75e-004	0.69
80° to 90° N	177	4.60	10.63	34.33	1.00e-006	0.01

Table 5. Depth distribution of non-zero biomass values. Mean, maximum (max), median and standard deviation (SD) of biomass (mg C m^{-3}) per depth interval, calculated from non-zero data points.

depth range (m)	entries	Mean (mg C m^{-3})	Max (mg C m^{-3})	Min (mg C m^{-3})	Median (mg C m^{-3})	SD
0–10	1806	20.65	5.45e+003	0	0.02	157.81
10–25	612	14.44	557.41	0	0.04	57.53
25–50	1296	3.25	434.37	0	0.002	18.26
50–200	7508	0.65	308.47	0	0.02	5.74
200–500	2028	0.19	9.85	0	0.002	1.04
500–2000	276	0.02	3.20	0	0.004	0.18

error, it is not a major source of bias in our analyses of geographic trends in pteropod biomass distribution.

3.3 Temporal distribution of data

Our database spans the period 1950–2010, and temporally, the data was fairly evenly distributed across all decades, with at least one sampling peak per decade. Several sampling peaks were recorded in the late 1950s, then in the 1960s–1970s, followed by high numbers of data from the early 1990s and 2000s. We recorded fewer samples in the 1980s (Fig. 6). To check for seasonal biases, the data was divided into four seasons for each hemisphere (Table 7). While in the NH, the data was distributed evenly across the four seasons (24 % in 335 spring, 23 % in summer, 24 % in autumn and 30 % in winter), sampling in the SH was biased towards winter and summer (30 % and 25 %, respectively), with much lower coverage during the other seasons (19 and 16 % in spring and fall, respectively).

3.4 Global biomass characteristics for all pteropod groups and for shelled-pteropods only

For all pteropod groups combined, the range of global biomass concentrations was wide, spanning over four orders of magnitude (Fig. 8a), with a mean and median biomass of 4.1 mg C m^{-3} (SD = 59.1) and 0.0083 mg C m^{-3} for all data points, and 4.6 mg C m^{-3} (SD = 62.5) and 0.0145 mg C m^{-3} for non-zero biomass values, respectively. In the NH, the mean biomass was 4.0 mg C m^{-3} (SD = 64.8) and the median biomass, 0.02 mg C m^{-3}. In the SH, the mean biomass was 8.15 mg C m^{-3} (SD = 45.4) and the median biomass 0.001 mg C m^{-3} (Table 3). Although the median biomass in the SH was one order of magnitude smaller than in the NH, the mean biomass in the SH was twice that of the NH.

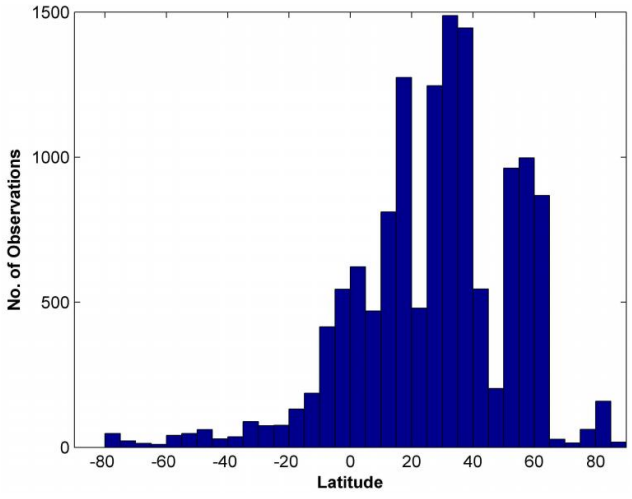

Figure 5. Number of pteropod observations as a function of latitude for the period 1950–2010.

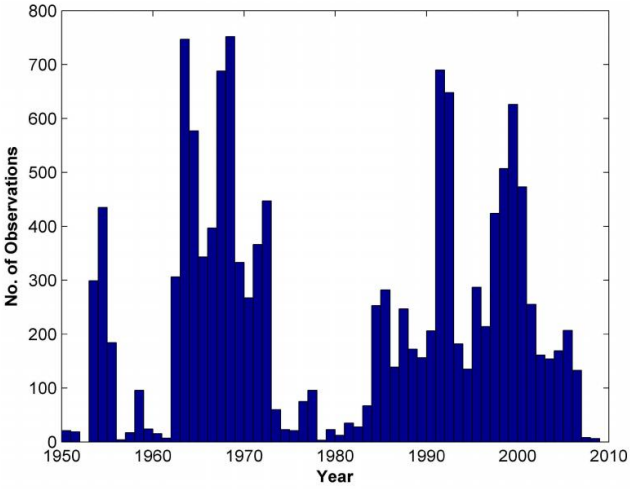

Figure 6. Number of observations per year, for the years 1950–2010.

For shelled pteropod groups only, the mean and median biomass for non-zero values was 3.81 mg C m^{-3} (SD = 40.24), and 0.0078 mg C m^{-3}, respectively, and the maximum biomass was 2979.7 mg C m^{-3}. Considering the mean biomass of shelled and non-shelled pteropods, shelled pteropods constitute 83 % to the total pteropod biomass, the remainder being made up of non-shelled pteropod taxa. When considered in terms of median biomass, 54 % was made up of shelled-pteropods and 46 % made up of non-shelled pteropods, indicating that the dominance of shelled-pteropods is in part due to the fact that they sometimes occur at very high concentrations.

Through assuming, firstly, an inorganic to organic carbon ratio of 0.27 : 0.73 (Bednaršek et al., 2012) and secondly an inorganic carbon to calcium carbonate molecular mass ratio of 8.33 (Eq. 10) gave a mean global carbonate biomass of 23.17 mg $CaCO_3$ m^{-3}, and a maximum biomass was 1.81 g $CaCO_3$ m^{-3}. These estimates were derived from non-zero biomass records only.

Table 6. Percentage distribution of non-zero data entries with respect to month for the Northern (NH) and Southern (SH) Hemispheres.

months	entries	NH season	SH season	% NH non-zero data	% SH non-zero data
January	1185	winter	summer	8.4	11.7
February	1457	winter	summer	9.4	20.7
March	998	spring	autumn	7.4	6.1
April	1298	spring	autumn	9.5	9.0
May	876	spring	autumn	6.9	3.7
June	802	summer	winter	6.4	4.1
July	1352	summer	winter	10.4	7.1
August	1790	summer	winter	13.1	13.8
September	1143	autumn	spring	8.4	9.0
October	1049	autumn	spring	8.4	3.7
November	859	autumn	spring	6.8	3.7
December	806	winter	summer	5.4	10.2

3.4.1 Latitudinal biomass distribution

Pteropods were found at all latitudes at which samples were taken (Figs. 5, 8a). The highest maximum, mean and median biomass values were located in the NH between 40 and 50° N (mean biomass of 5.42 mg C m^{-3} (SD = 79.94), median biomass of 0.06 mg C m^{-3}). The highest mean and median biomass values in the SH were located between 70 and 80° S (39.71 mg C m^{-3} (SD = 93.00) and 0.009 mg C m^{-3}, respectively; Table 3). However, relatively high biomasses were not restricted to a particular latitude or ocean basin but were widespread, including high-latitudinal, temporal and equatorial regions in the both hemispheres. The only exception was the latitudinal band between 20 and 40° in the NH and SH, where biomass was considerably lower (Fig. 8). There was a difference in latitudinal trends between hemispheres (Fig. 9a, b), with highest biomass values in the NH being at mid-latitudes decreasing towards the equator and the poles, while, in the SH, highest biomass values were seen at the poles and steadily decreasing through the mid-latitudes towards the equator. Biomass values at both poles were within the same order of magnitude.

3.4.2 Depth distribution

Pteropods were observed at all depths down to 2000 m, although the funnel-shaped biomass pattern from the surface towards the depth indicates a sharp decrease in biomass below 200 m (Fig. 8b). The highest values were recorded at the surface (0–10 m), with a mean biomass of 20.65 mg C m^{-3} (SD = 157.81) and median biomass of 0.02 mg C m^{-3}. Mean

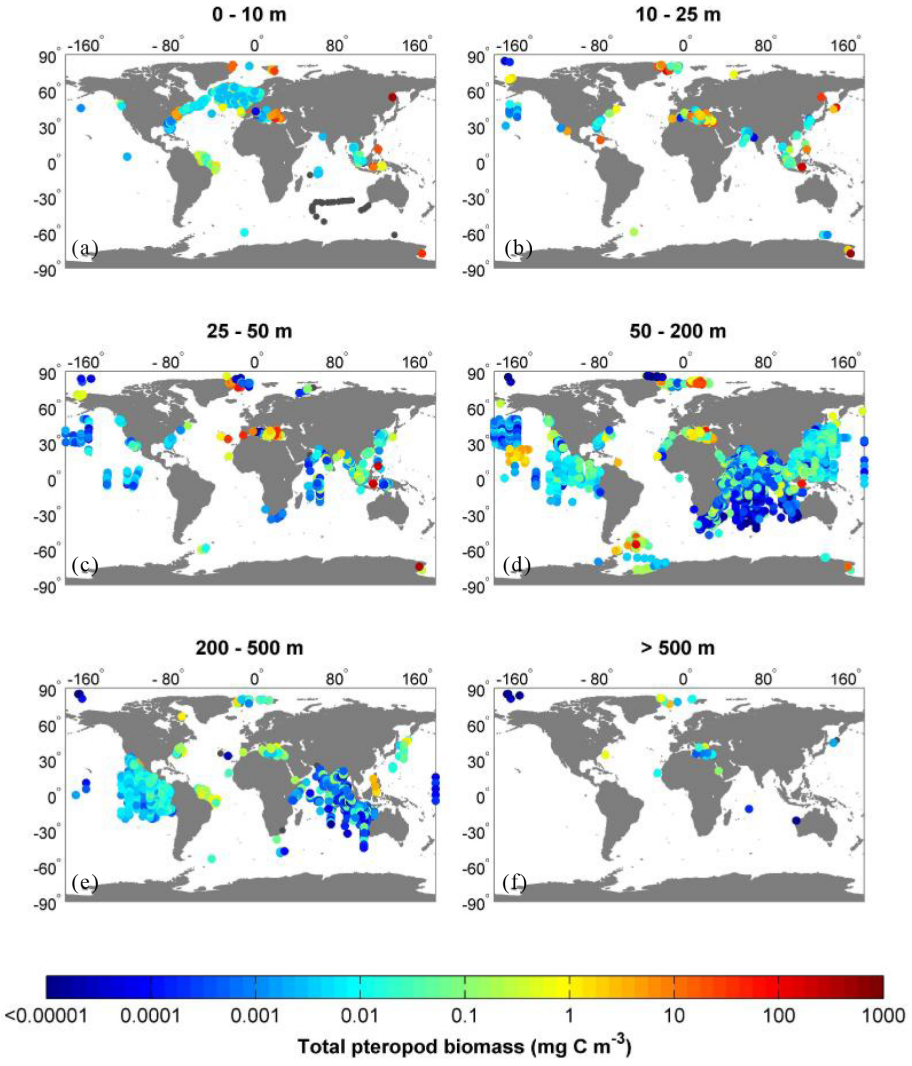

Figure 7. Pteropod carbon biomass (mg C m^{-3}) for six depth intervals: **(a)** surface (0–10 m), **(b)** 10–25 m, **(c)** 25–50 m, **(d)** 50–200 m, **(e)** 200–500 m, **(f)** ≥ 500 m.

and median biomass gradually decrease with the depth by one order of magnitude from 10 to 200 m, and by two orders of magnitude between the 10–200 m and 200–2000 m depth bands (Table 5, Fig. 8b).

The pattern of pteropod distribution demonstrates that higher abundances are closely related to continental shelves and areas of high productivity or nutrient loads (Fig. 7). This can be particularly exemplified in the eastern North Pacific central water, which is a rather small area affected by the inflow from the more productive transitional and equatorial adjacent areas (Longhurst, 2007), with a three to four magnitude higher biomass, in comparison to the surrounding areas.

In all ocean basins, biomass levels above 100 mg C m^{-3} only occurred in the 0–200 m depth layers. However, in tropical regions, some of the highest biomass levels were found in the 200–500 m depth strata, where concentrations typically reached between 1 and 10 mg C m^{-3} (Fig. 7). This suggests that tropical species concentrate at deeper depths than temperate and high-latitude species. Such geographic patterns in the depth distribution of pteropods have previously been noted by Solis and von Westernhagen (1978), Wormuth (1981) and Almogi-Labin et al. (1998).

3.4.3 Seasonal distribution of pteropod biomass

Seasonal variations in biomass values were much more extreme in the SH compared to the NH, although it is to be noted that sample coverage was comparatively greater in the NH (Table 7, Fig. 9). In both hemispheres, mean biomass peaked in the spring. However, the peak was an order of magnitude higher in the SH compared to the NH (Table 7). The ratio between spring and winter biomass was approximately 2 : 1 in the NH, but around 1300 : 1 in the SH. The difference in ratios is mainly explained by the virtual disappearance of

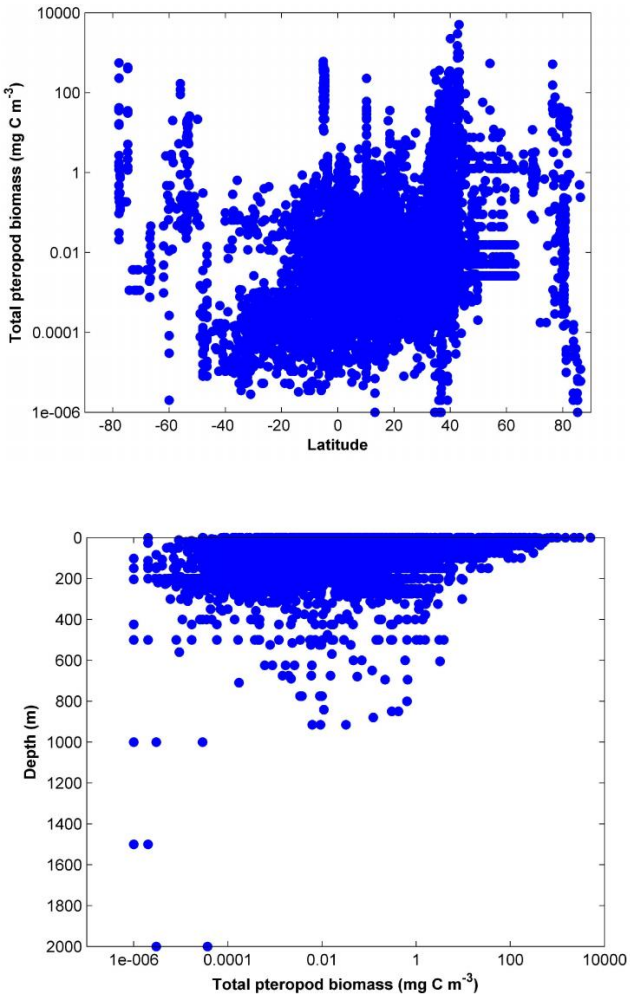

Figure 8. (Above) the distribution of pteropod biomass (mg C m^{-3}) as a function of latitude; (below) the relationship between pteropod biomass and net-capture depth.

pteropods in the SH during winter. Biomass levels were relatively similar between the NH and SH during summer and autumn. The seasonal peaks and troughs in mean biomass in both hemispheres correspond to a life-history pattern of spring spawning, probably in response to seasonal pulses of productivity, as described by Hunt et al. (2008) and Bednaršek et al. (2012).

Despite the seasonal peaks and troughs in biomass, a residual biomass level was always present (Fig. 9). This indicates that there must be a degree of overlap in generations (Bednaršek et al., 2012). In the higher latitudes, where there is likely just a single recruitment event per year, meaning that these pteropods must have a life-cycle that extends into a second year. In the Southern Ocean, Bednaršek et al. (2012) proposed that some *Limacina helicina ant.* lived for more than 2 yr and, although small in number, these individuals may be vital for future recruitment. Strong seasonality increases the vulnerability of early life-stages of pteropods that rely on pulses of production to thrive (Bernard and Froneman, 2009; Seibel and Dierssen, 2003). An overlap of generations gives populations greater stability in temporally variable environments.

3.4.4 Global estimates of the pteropod biomass stock and productivity

Given representative data coverage at the both hemispheres, global mean pteropod biomass of 0.0046 g C m^{-3} (SD = 62.5) was calculated for any point of time. To extrapolate from regional to global pteropod biomass, pteropod depth distribution and absolute area of the global ocean are required. With regards to depth distribution, Fig. 8a is indicative of pteropod biomass to be uniformly distributed within the upper 300 m, and two orders of magnitude less abundant below 300 m. The 300-m depth level was hence taken as a conservative estimate of their overall occurrence. Considering the absolute surface area of the global deep ocean (Milliman and Droxler, 1996; total area equals 362.03×10^6 km^2 cf. Dietrich et al., 1975), two values were taken to determine global pteropod biomass: the global ocean surface excluding shelf seas (322×10^6 km^2) was taken as a minimum area inhibited by pteropods, while the total ocean surface area was determined as a maximum (362.03×10^6 km^2). Considering minimum and maximum area inhabited by pteropods, global pteropod biomass ranges from 444 to 505 Tg of C at any point in time. This range of estimates, based on the observational results is similar to pteropod productivity estimate of 0.87 Pg C yr^{-1} obtained through modelling work by Gangstø et al. (2008). Lebrato et al. (2010) estimated global carbon productivity budget to range between 0.96 and 2.56 Pg C yr^{-1}. This indicates that pteropods contribute 20–42 % towards global carbonate budget.

The average turnover time is known to be different for various species, shorter (several months) for tropical species and longer (more than one year) for the high-latitudinal species (Lalli and Gilmer, 1989). Here, as reported in several papers (Van der Spoel, 1973; Wells Jr., 1976; Hunt et al., 2008; etc.), the average pteropods turnover time was assumed to be one year, with high latitudinal species to be exceptions (e.g. Bednaršek et al., 2012) and recorded the life cycle of *Limacina helicina antarctica* to span over 3 yr. At a global scale, and an average annual distribution, the entire pteropod production would hence amount to 444–505 Tg C yr^{-1}, which is about five times the estimated planktic foraminifers biomass production (Schiebel and Movellan, 2012: 25–100 Tg C yr^{-1}), more than double of the estimated diazotroph biomass (Luo et al., 2012: 40–200 Tg C), and around one fifth of the total diatom production (Leblanc et al., 2012: 500–3000 Tg C). Comparing global pteropod to coccolithophorid carbon productivity (Balch et al., 2007), coccolithophorid production are approximately 1.5 to 3 times higher than our estimated pteropod production.

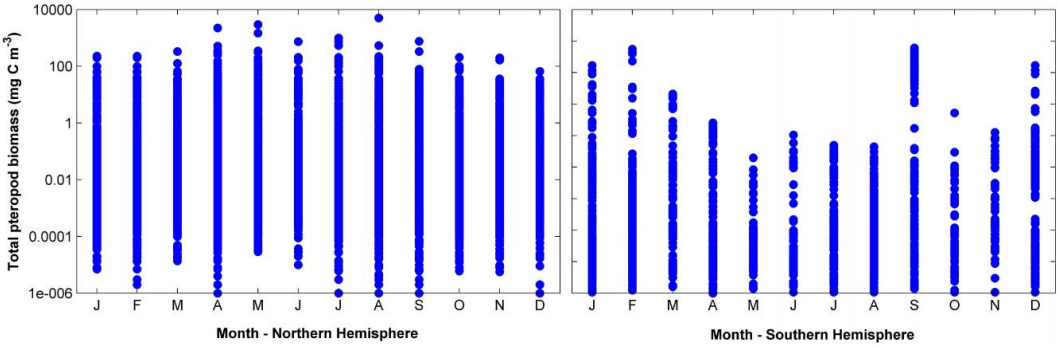

Figure 9. Distribution of pteropod biomass values (mg C m^{-3}) with respect to month, in the Northern Hemisphere (left) and Southern Hemisphere (right).

Table 7. Biomass (mg C m^{-3}) with respect to season for the Northern (NH) and Southern (SH) Hemispheres, showing the calculated mean, standard deviation (SD), median, minimum (min) and maximum (max). Biomass statistics are based on non-zero data entries only.

	NH mean	NH SD	NH median	NH min	NH max	SH mean	SH SD	SH median	SH min	SH max
winter	2.77	15.63	0.02	1e-006	557.41	0.03	0.09	4.54e-004	2.00e-006	1.06
spring	5.42	79.94	0.06	1e-006	3.0e+003	39.71	93.00	0.009	7.50e-006	608.35
summer	4.32	92.69	0.02	1e-006	5.05e+003	3.73	32.83	0.002	3.00e-006	557.41
autumn	2.44	18.39	0.03	1e-006	765.24	0.51	2.47	7.28e-004	3.30e-006	21.05

4 Discussion and conclusions

The aim of this study was to collect and synthesise available existing abundance and biomass data to generate the first global pteropod biomass database. Most studies reported abundance rather than biomass data, making it necessary to estimate carbon biomass using length to weight conversions and introducing levels of uncertainty as a result. Further uncertainties in the biomass estimates in this study will result from sampling errors such as net-escapement and net-avoidance, the variation in size classes between different pteropod species and generations. Further considerations around these uncertainties are discussed below.

With regards to the sampling error, the use of different nets for different pteropod size classes generates uncertainty, as the capture and filtering efficiencies differ between nets. Furthermore, sampling issues such as net-avoidance behaviour, extrusion of animals through mesh and clogging of the net (Harris et al., 2000) will influence abundance measurements. In addition, there is generally an insufficient use of smaller meshed nets to estimate population size. Wells Jr. (1973) proposed that there was a clear underestimation of the fraction of the pteropod population smaller than 100 μm. As they constitute by far the most numerous part of the natural population (Fabry, 1989), there is a clear under-representation of this cohort in the scientific literature and thus of their importance within the microzooplankton community (Dadon and Masello, 1999). When sampling with small vertical nets, which preferentially catch small or sluggish taxa, additional sampling errors arise from the fact that the nets can be avoided by larger plankton. On the other hand, nets with larger mesh size can miss the mesozooplankton size fractions including pteropods (Boysen-Ennen et al., 1991). We tried to address potential biases through systematic examination of mesh sizes, net types and sampling strategies (wherever available in the literature) relative to biomass estimates. Our analyses indicated, firstly, that most biomass lay within the mid-size ranges, meaning that the undersampling of smaller organisms by some studies is unlikely to have a large impact on biomass estimates. Secondly, there was no geographic bias in the use of different nets and meshes, indicating that sampling error is unlikely to bias analyses of geographic trends in biomass. Overall, we conclude that the documented variation in mesh size between studies included within the database was not a source of a large-scale bias within global biomass patterns. Therefore, although users of the database must be vigilant with regards to this potential source of error, we believe that the inclusion of all data, irrespective of the mesh size and sampling strategy used, maximises the potential insights that can be gained from this database.

There were a number of sources of uncertainty in deriving biomass values from the majority of studies within the database that only provided abundance data. To convert from abundance to biomass requires knowledge of the length distribution of specimens but neither this data, nor the respective life-stages of specimens were commonly reported. Where such information was not given, we assumed that all specimens were adults and used literature based estimated of body

length. This approach probably resulted in an overestimation of biomass, given that at least part of the sampled population may have been smaller juvenile stages. Furthermore, where sizes were reported, there was often a lack of further statistical descriptors such as minimum or maximum length, so preventing levels of variance in biomass to be estimated. For some species, there was no available length to weight conversions and so more generic algorithms were applied based on the shape and morphological features (shelled/non-shelled) of the organisms, following the approach of GLOBEC (Little and Copley, 2003). This approach no doubt introduced further errors although there is little alternative to the use of such generic functions until a more systematic documentation of the length and weight characteristics of a wider range of pteropod species is undertaken.

The seasonal spread of sampling was much more even in the NH compared to the SH. Whereas we were able to document how patterns of biomass shifted geographically between seasons in the NH, our ability to achieve this was far more constrained in the SH. In particular, sampling in winter and spring was particularly sparse in the SH. It is important that future sampling efforts in that hemisphere concentrate on these less sampled times of year.

This study has enabled estimates of global pteropod biomass across a number of spatial and temporal scales. Furthermore, it has revealed some global patterns of pteropod biomass, only possible due to the wealth of data available in our data sets. Also, calculating the biomass of shelled pteropods only, we have estimated the contribution of this group to the global carbonate inventory. This database has the potential be a valuable tool for future modelling work, both of ecosystem processes and for the study of global biogeochemical cycles, since pteropods are a major contributor to organic and inorganic carbon fluxes. It can also make a timely contribution to the assessment of the effects of ocean acidification, particularly in terms of the vulnerability of calcifying species, since it provides a benchmark against which model projections and future sampling efforts can be compared.

Appendix A

A1 Available dataset at PANGEA

A full data set containing all abundance/biomass data points can be downloaded from the data archive PANGAEA, The data file contains longitude, latitude, sampling depth (m), date (Year, Month, Day in ISO format), taxon/species/body size, abundance (ind. m^{-3}), biomass (C mg m^{-3}), mesh size (μm), sampling strategy and full data reference list (doi/journal/database) doi:10.1594/PANGAEA.777387.

A2 Gridded NetCDF biomass product

The biomass data has been gridded onto a $360 \times 180°$ grid, with a vertical resolution of 33 WOA depth levels. Data has been converted to NetCDF format for easy use in model evaluation exercises. The NetCDF file can be downloaded from PANGAEA (doi:10.1594/PANGAEA.777387). It contains data on longitude, latitude, sampling depth (m), month, abundance (ind. m^{-3}) and biomass (mg C m^{-3}).

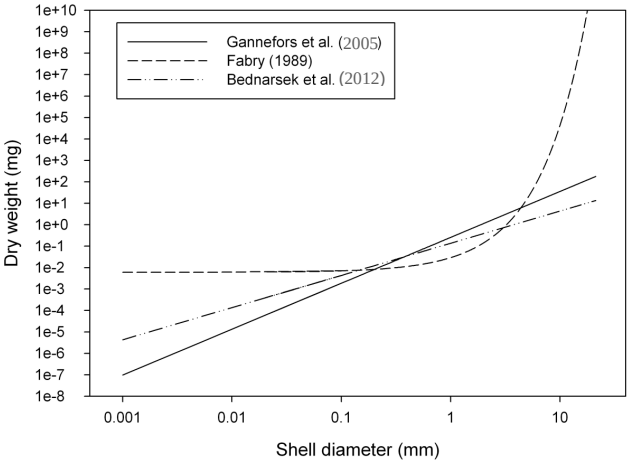

Figure B1. Shell diameter to dry weight relationships for *Limacina helicina* derived by three different studies.

Table C1. Body dimensions and shapes of a range of shelled and non-shelled pteropod species (source: Marine identification portal (http://species-identification.org/), except for *Clione limacina** – Böer et al., 2005).

Order	Suborder	Taxon	Subspecies/ Formae	Mean shell length (mm)	Mean shell width (mm)	Body length (mm)	Shell/body shape	Additional information	Group
Thecosomata	Euthecosomata	*Limacina helicina*	*helicina helicina*	6	8		round	left coiled shell, moderately highly spired, aperture higher than wide, height/diameter ration=0.75	Round/cylindrical/ globular
Thecosomata	Euthecosomata	*Limacina helicina*	*helicina pacifica*	5	2				Round/cylindrical/ globular
Thecosomata	Euthecosomata	*Limacina retroversa*	*retroversa*	2.5	2.6		round	small, left coiled shell, no umbilical keel, spire moderately highly coiled	Round/cylindrical/ globular
Thecosomata	Euthecosomata	*Limacina bulimoides*		2	1.4		round	highly coiled spire	Round/cylindrical/ globular
Thecosomata	Euthecosomata	*Limacina inflata*			1.3		round	coiled nearly in one level; average shell diameter =0.86, aperture length=0.68 mm, diameter of operculum=0.31 mm, aperture breadth=0.5 mm	Round/cylindrical/ globular
Thecosomata	Euthecosomata	*Limacina helicina*	*antarctica*		5		round	left coiled, spire variable	Round/cylindrical/ globular
Thecosomata	Euthecosomata	*Limacina helicina*	*antarctica antarctica rangii*	2	3.5				Round/cylindrical/ globular
Thecosomata	Euthecosomata	*Limacina trochiformis*		1	0.8		round	left coiled, apical angle 75–96°	Round/cylindrical/ globular
Thecosomata	Euthecosomata	*Limacina helicina* spp. *average*			4.22				Round/cylindrical/ globular
Thecosomata	Euthecosomata	*Limacina trochiformis*		1	0.8		round	left coiled, apical angle 75–96°	Round/cylindrical/ globular
Thecosomata	Euthecosomata	*Limacina lesueuri*		0.8	1		round	flatly left coiled, spire depressed; max diameter of operculum = 0.6 mm and length/width ratio=2/3	Round/cylindrical/ globular
Thecosomata	Euthecosomata	*Limacina* spp.			2.98			the length calculated as the average of all species	Round/cylindrical/ globular
Gymnosomata		*Clione limacina*	*limacina antarctica*		25	Up to 40	barrel	body pointed posteriorly	Barrel/oval-shaped (naked)
Gymnosomata		*Clione limacina*	*limacina meridionalis*		21	20	barrel	Cone elongated	Barrel/oval-shaped (naked)
Gymnosomata		*Clione limacina**			12				Barrel/oval-shaped (naked)
Gymnosomata		*Clione limacina larvae*			0.3				
Gymnosomata		*Clione* spp.			14.57			the length calculated as the average of all species	Barrel/oval-shaped (naked)
Thecosomata	Euthecosomata	*Hyalocylis striata*		8		up to 8	cylindrical	uncoiled, cross-section round, shell curved faintly dorsally; rear angle of adult shell 24°	Cone-shaped (needle/tube/bottle)

Table C1. Continued.

Order	Suborder	Taxon	Subspecies/ Formae	Mean shell length (mm)	Mean shell width (mm)	Body length (mm)	Shell/body shape	Additional information	Group
Thecosomata	Euthecosomata	*Styliola subula*		13		13	needle-like	shell is (conical), uncoiled, the cross-section is round, long, tubular, not curved; rear angle of shell is 11°	Cone-shaped (needle/tube/bottle)
Gymnosomata		*Spongiobranchaea australis*		20		max 22	oval	long body	Barrel/oval-shaped (naked)
Gymnosomata		*Spongiobrachaea australis juv.*		10					Barrel/oval-shaped (naked)
Gymnosomata		*Spongiobranchaea* spp.		15					Barrel/oval-shaped (naked)
Gymnosomata		*Pneumodermopsis*	*teschi*			up to 9.1	barrel		Barrel/oval-shaped (naked)
Gymnosomata		*Pneumodermopsis*	*pulex*			up to 8	barrel		Barrel/oval-shaped (naked)
Gymnosomata		*Pneumodermopsis*	*macrochira*			up to 2	barrel		Barrel/oval-shaped (naked)
Gymnosomata		*Pneumodermopsis*	*ciliata*			up to 15	barrel	slender body	Barrel/oval-shaped (naked)
Gymnosomata		*Pneumodermopsis*	*spoeli*			up to 3 (2.6)	barrel	body rounded then contracted	Barrel/oval-shaped (naked)
Gymnosomata		*Pneumodermopsis*	*simplex*			up to 5 (4.5)	barrel		Barrel/oval-shaped (naked)
Gymnosomata		*Pneumodermopsis*	*paucidens*			up to 5	barrel		Barrel/oval-shaped (naked)
Gymnosomata		*Pneumodermopsis*	*canephora*			up to 12	barrel		Barrel/oval-shaped (naked)
Gymnosomata		*Pneumodermopsis*	*polycotyla*			up to 5	barrel		Barrel/oval-shaped (naked)
Gymnosomata		*Pneumodermopsis* spp.				6.5		the length calculated as the average of all species	Barrel/oval-shaped (naked)
Gymnosomata		*Paedocline*	*doliiformis*	1.5				elongate oval to cylindrical shape	Barrel/oval-shaped (naked
Thecosomata	Euthecosomata	*Cavolinia globulosa*		6	4.5		globular		Triangular/pyramidal
Thecosomata	Euthecosomata	*Cavolinia inflexa*	*inflexa*	7	5	6	triangular		Triangular/pyramidal
Thecosomata	Euthecosomata	*Cavolinia inflexa*	*imitans*	8			triangular		Triangular/pyramidal
Thecosomata	Euthecosomata	*Cavolinia inflexa*	*labiata*	8	5.5		triangular		Triangular/pyramidal
Thecosomata	Euthecosomata	*Cavolinia longirostris*	*f. longirostris*	6.2	6.8–4.9	7	triangular	accepted name *Dicavolinia longirostris*	Triangular/pyramidal
Thecosomata	Euthecosomata	*Cavolinia longirostris*	*f. angulosa*	3.9	3.7–2.3	5	triangular	accepted name *Dicavolinia longirostris*	Triangular/pyramidal
Thecosomata	Euthecosomata	*Cavolinia longirostris*	*f. strangulata*	4	4.1–2.7	5	triangular	accepted name *Dicavolinia longirostris*	Triangular/pyramidal
Thecosomata	Euthecosomata	*Cavolinia uncinata*	*uncinata uncinata*	6.5	4.0–6.6	8	triangular	uncoiled shell	Triangular/pyramidal
Thecosomata	Euthecosomata	*Cavolinia uncinata*	*uncinata f. pulsatapusilla*	6.1	9.5		triangular		Triangular/pyramidal
Thecosomata	Euthecosomata	*Cavolinia* spp.		6.2				the length calculated as the average of all species	Triangular/pyramidal
Thecosomata	Euthecosomata	*Clio convexa*		8	4.5	up to 8	pyramidal	shell uncoiled	Triangular/pyramidal

Table C1. Continued.

Order	Suborder	Taxon	Subspecies/ Formae	Mean shell length (mm)	Mean shell width (mm)	Body length (mm)	Shell/body shape	Additional information	Group
Thecosomata	Euthecosomata	*Clio cuspidata*		20	30	up to 20	pyramidal	shell uncoiled	Triangular/pyramidal
Thecosomata	Euthecosomata	*Clio piatkowskii*		13.5	16	14	broad pyramidal		Triangular/pyramidal
Thecosomata	Euthecosomata	*Clio pyramidata*		20	10		pyramidal		Triangular/pyramidal
Thecosomata	Euthecosomata	*Clio pyramidata*	*martensi*	17					Triangular/pyramidal
Thecosomata	Euthecosomata	*Clio pyramidata*	*antarctica*	17					Triangular/pyramidal
Thecosomata	Euthecosomata	*Clio pyramidata*	*lanceolata*	20					Triangular/pyramidal
Thecosomata	Euthecosomata	*Clio pyramidata* spp.		18.5					Triangular/pyramidal
Thecosomata	Euthecosomata	*Clio* spp.		16.5				the length calculated as the average of all species	Triangular/pyramidal
Thecosomata	Euthecosomata	*Creseis acicula*	*acicula*	33	1.5		tube	shell is not curved, cross-section circular, extremely long and narrow, aperture rounded, rear angle of shell 13–14°	Cone-shaped (+needle/ tube/bottle)
Thecosomata	Euthecosomata	*Creseis acicula*	*clava*	6					Cone-shaped (+needle/ tube/bottle)
Thecosomata	Euthecosomata	*Creseis acicula* spp.		19.5					Cone-shaped (+needle/ tube/bottle)
Thecosomata	Euthecosomata	*Creseis virgula*	*virgula*	6	max 2	6	tube	shell is curved (distinctly curved dorsally), uncoiled, long and narrow	Cone-shaped (+needle/ tube/bottle)
Thecosomata	Euthecosomata	*Creseis virgula*	*conica*	7	aperture-diameter =1 mm	up to 7	tube	shell curved and slender, cross-section is round	Cone-shaped (+needle/ tube/bottle)
Thecosomata	Euthecosomata	*Creseis virgula*	*constricta*	3.5	0.4	4	tube	uncoiled shell, cross-section round, short and narrow, slightly curved	Cone-shaped (+needle/ tube/bottle)
Thecosomata	Euthecosomata	*Creseis virgula* spp.		5.5	0.2		tube		Cone-shaped (+needle/ tube/bottle)
Thecosomata	Euthecosomata	*Creseis* spp.		11.5				the length calculated as the average of all species	Cone-shaped (+needle/ tube/bottle)
Thecosomata	Euthecosomata	*Cuvierina columnella*	*columnella*	10	3	up to 10	bottle-shaped	the greatest shell width is found at less than 173 of the shell length from posterior	Cone-shaped (+needle/ tube/bottle)
Thecosomata	Euthecosomata	*Diacria costata*		2.3	1.7–2.2	3	globular	shell uncoiled	Triangular/pyramidal
Thecosomata	Euthecosomata	*Diacria danae*		1.7	1.1–1.7	2	globular	shell uncoiled	Triangular/pyramidal
Thecosomata	Euthecosomata	*Diacria quadridentata*		3	1.8–2.5	2	globular	shell uncoiled	Triangular/pyramidal

Table C1. Continued.

Order	Suborder	Taxon	Subspecies/ Formae	Mean shell length (mm)	Mean shell width (mm)	Body length (mm)	Shell/body shape	Additional information	Group
Thecosomata	Euthecosomata	*Diacria rampali*		9.5	9	9	cone-shaped	bilateral symmetrical, uncoiled shell, slender, long caudal spine; spine mark width=0.95 mm, aperture height=0.95.	Triangular/pyramidal
Thecosomata	Euthecosomata	*Diacria trispinosa*	*trispinosa*	8	10	1	cone-shaped	bilateral symmetrical, uncoiled shell, long caudal spine; the ration upperlip-spine tip/spine tip-membrane=1.3, spine mark width=1.5 mm, aperture height=0.9 mm.	Triangular/pyramidal
Thecosomata	Euthecosomata	*Diacria major*		10.7	11			uncoiled bilateral symmetrical, long caudal spine; ratio upperlip-spine tip/spine-tip membrane=1,.65 mm, spine mark width=1.2 mm, aperture height=1 mm;	Triangular/pyramidal
Thecosomata	Euthecosomata	*Diacria* spp.		5.9				the length calculated as the average of all species	Triangular/pyramidal
THECOSOMATA COMBINED				8.1				shelled	
GYMNOSOMATA COMBINED						12.0		naked	
PTEROPODA COMBINED				8.9				shelled	

Acknowledgements. We thank K. Blachowiak-Samolyk, E. Boysen-Ennen, E. A. Broughton, C. Clarke, M. Daase, V. G. Dvoretsky, T. D. Elliot, H. Flores, B. A. Foster, P. W. Froneman, B. P. V. Hunt, L. Mousseau, J. Nishikawa, M. D. Ohman, T. O'Brien, E. A. Pakhomov, L. Pane, M. Fernandez de Puelles, K. A. Rogachev, P. H. Schalk, N. Solis, K. M. Swadling, A. F. Volkov, P. Ward, I. Werner, J. H. Wormuth for a permission to use and republish their data on pteropods in the MAREDAT project and this paper.

The lead author is grateful to R. A. Feely (NOAA) and R. Schiebel (Université d'Angers-BIAF) for their invaluable advice and ideas. Thanks also go to Marko Vuckovic from the University of Nova Gorica for the help with the Matlab software changes. The work at ETH for NB was partly funded through an Erasmus scholarship. GT was supported by the Ecosystems core research programme at the British Antarcttic Survey. The research leading to these results has received funding from the European Community's Seventh Framework Programme (FP7 2007–2013) under grant agreement no. 238366.

Edited by: W. Smith

References

Almogi-Labin, A., Hemleben, C., and Meischner, D.: Carbonate preservation and climatic changes in the central Red Sea during the last 380 kyr as recorded by pteropods, Marine Micropaleontology, 33, 87–107, doi:10.1016/S0377-8398(97)00034-0, 1998.

Acker, J. G. and Byrne, R. H.: The influence of surface state and saturation state on the dissolution kinetics of biogenic aragonite in seawater, Am. J. Sci., 289, 1098–1116, 1989.

Andersen, V., Sardou, J., and Gasser, B.: Macroplankton and micronekton in the northeast tropical Atlantic: abundance, community composition and vertical distribution in relation to different trophic environments, Deep-Sea Res. Pt. I, 44, 193–222, doi:10.1016/S0967-0637(96)00109-4, 1997.

Bednaršek, N., Tarling, G., Fielding, S., and Bakker, D.: Population dynamics and biogeochemical significance of *Limacina helicina antartica* in the Scotia Sea (Southern Ocean), Deep-Sea Res. Pt. II, 59–60, 105–116, doi:10.1016/j.dsr2.2011.08.003, 2012.

Bernard, K. S. and Froneman, P. W.: Trophodynamics of selected mesozooplankton in the west-Indian sector of the Polar Frontal Zone, Southern Ocean, Polar Biol., 28, 594–606, doi:10.1007/s00300-005-0728-3, 2005.

Bernard, K. S. and Froneman, P. W.: The sub-Antarctic euthecosome pteropod, *Limacina retroversa*: Distribution patterns and trophic role, Deep-Sea Res. Pt. I, 56, 582–598, doi:10.1016/j.dsr.2008.11.007, 2009.

Berner, R. A. and Honjo, S.: Pelagic sedimentation of aragonite: its geochemical significance, Science, 211, 940–942, 1981.

Blachowiak-Samolyk, K., Søreide, J. E., Kwasniewski, S., Sundfjord, A., Hop, H., Falk-Petersen, S., and Hegseth, E. N.: Hydrodynamic control of mesozooplankton abundance and biomass in northern Svalbard waters (79–81° N), Deep-Sea Res. Pt. II, 55, 2210–2224, 2008.

Böer, M., Gannefors, C., Kattner, G., Graeve, M., Hop, H., and Falk-Petersen, S.: The Arctic pteropod *Clione limacina*: seasonal lipid dynamics and life-strategy, Mar. Biol., 147, 707–717, 2005.

Boysen-Ennen, E., Hagen, W., Hubold, G., and Piatkowski, U.: Zooplankton biomass in the ice-covered Weddell Sea, Antarctica, Mar. Biol., 111, 227–235, 1991.

Broughton, E. A. and Lough, R. G.: A direct comparison of MOCNESS and Video Plankton Recorder zooplankton abundance estimates: Possible application for augmenting net sampling with video systems, Deep-Sea Res. Pt. II, 53, 2789–2807, doi:10.1016/j.dsr2.2006.08.013, 2006.

Buitenhuis, E. T., Vogt, M., Moriarty, R., Bednaršek, N., Doney, S. C., Leblanc, K., Le Quéré, C., Luo, Y.-W., O'Brien, C., O'Brien, T., Peloquin, J., Schiebel, R., and Swan, C.: MAREDAT: towards a World Ocean Atlas of MARine Ecosystem DATa, Earth Syst. Sci. Data Discuss., 5, 1077–1106, doi:10.5194/essdd-5-1077-2012, 2012.

Clarke, C. and Roff, J. C.: Abundance and Biomass of Herbivorous Zooplankton off Kingston, Jamaica, with Estimates of their Annual Production, Estuar. Coast. Shelf S., 31, 423–437, 1990.

Daase, M. and Eiane, K.: Mesozooplankton distribution in northern Svalbard waters in relation to hydrography, Polar Biol., 30, 969–981, doi:10.1007/s00300-007-0255-5, 2007.

Dadon, J. R. and Masello, J. F.: Mechanisms generating and maintaining the admixture of zooplanktonic molluscs (Euthecosomata: Opistobranchiata: Gastropoda) in the Subtropical Front of the South Atlantic, Mar. Biol., 135, 171–179, 1999.

Davis, C. S. and Wiebe, P. H.: Macrozooplankton Biomass in a Warm-Core Gulf Stream Ring: Time Series Changes in Size Structure, Taxonomic Composition, and Vertical Distribution, J. Geophys. Res., 90, 8871–8884, 1985.

Dietrich, G., Kalle, K., Krauss, W., and Siedler, G.: Allgemeine Meereskunde, 3, Auflage, Gebruder Borntrager, Berlin, Stuttgart, 593 pp., 1975.

Dvoretsky, V. G. and Dvoretsky, A. G.: Summer mesozooplankton distribution near Novaya Zemlya (eastern Barents Sea), Polar Biol., 32, 719–731, doi:10.1007/s00300-008-0576-z, 2009.

Elliot, T. D., Tang, K. W., and Shields, A. R.: Mesozooplankton beneath the summer sea ice in McMurdo Sound, Antarctica: abundance, species composition and DMSP content, Polar Biol., 32, 113–122, doi:10.1007/s00300-008-0511-3, 2009.

Fabry, V. J.: Aragonite production by pteropod molluscs in the subarctic Pacific, Deep-Sea Res., 36, 1735–1751, doi:10.1016/0198-0149(89)90069-1, 1989.

Fernandez de Puelles, M. L., Alemany, F., and Jansa, J.: Zooplankton time-series in the Balearic Sea (Western Mediterranean): Variability during the decade 1994–2003, Prog. Oceanogr., 74, 329–354, doi:10.1016/j.pocean.2007.04.009, 2007.

Flores, H., van Franeker, J.-A., Cisewski, B., Leach, H., van de Putte, A. P., Meesters, E. H. W. G., Bathmann, U., and Wolff, W. J.: Macrofauna under sea ice and in the open surface layer of the Lazarev Sea, Southern Ocean, Deep-Sea Res. Pt. II, 58, 1948–1961, doi:10.1016/j.dsr2.2011.01.010, 2011.

Foster, B. A.: Composition and Abundance of Zooplankton Under the Spring Sea Ice of McMurdo Sound, Antarctica, Polar Biol., 8, 41–48, 1987.

Froneman, P. W., Pakhomov, E. A., and Treasure, A.: Trophic importance of the hyperiid amphipod, *Themisto gaudichaudi*, in the Prince Edward Archipelago (Southern Ocean), Polar Biol., 23, 429–436, 2000.

Gannefors, C., Böer, M., Kattner, G., Graeve, M., Eiane, K., Gulliksen, B., Hop, H., and Falk-Petersen, S.: The Arctic sea butterfly *Limacina helicina*: lipids and life strategy, Mar. Biol., 147, 169–177, doi:10.1007/s00227-004-1544-y, 2005.

Gangstø, R., Gehlen, M., Schneider, B., Bopp, L., Aumont, O., and Joos, F.: Modeling the marine aragonite cycle: changes under rising carbon dioxide and its role in shallow water $CaCO_3$ dissolution, Biogeosciences, 5, 1057–1072, doi:10.5194/bg-5-1057-2008, 2008.

Gilmer, R. W.: In situ observations of feeding in thecosomatous pteropod molluscs, Am. Malacol. Bull., 8, 53–59, 1990.

Gilmer, R. W. and Harbison, G. R.: Diet of *Limacina helicina* (Gastropoda: Thecosomata) in Arctic waters in midsummer, Mar. Ecol.-Prog. Ser., 77, 125–134, 1991.

Glover, D. M., Jenkinds, W. J., and Doney, S. C.: Modelling Methods for Marine Science, Cambridge University Press, Cambridge, UK, ISBN 978-0-521-86783-2, 2011.

Harbison, G. R. and Gilmer, R. W.: Swimming, buoyancy and feeding in shelled pteropods: a comparison of field and laboratory observations, J. Mollus. Stud., 58, 337–339, doi:10.1093/mollus/58.3.337, 1992.

Harris, R. P., Wiebe, P. H., Lenz, J., Skjoldal, H.-R., and Huntley, M.: Zooplankton methodology manual, Elsevier Academic Press, London, UK, 684 pp., 2000.

Hopkins, T. L.: Midwater food web in McMurdo Sound, Ross Sea, Antarctica, Mar. Biol., 96, 93–106, doi:10.1007/BF00394842, 1987.

Hunt, B. P. V. and Hosie, G. H.: The seasonal succession of zooplankton in the Southern Ocean south of Australia, part I: The seasonal ice zone, Deep-Sea Res. Pt. I, 53, 1182–1202, doi:10.1016/j.dsr.2006.05.001, 2006.

Hunt, B. P. V., Pakhomov, E. A., Hosie, G. W., Siegel, V., Ward, P., and Bernard, K.: Pteropods in Southern Ocean ecosystems, Prog. Oceanogr., 78, 193–221, doi:10.1016/j.pocean.2008.06.001, 2008.

Jackson, G. A., Najjar, R. G., and Toggweiler, J. R.: Flux feeding as a mechanism for zooplankton grazing and its implications for vertical particulate flux, Limnol. Oceanogr., 38, 1328–1332, 1993.

Karnovsky, N. J., Hobson, K. A., Iverson, S., and Hunt Jr., G. L.: Seasonal changes in the diets of seabirds in the North Water Polynya: a multiple-indicator approach, Mar. Ecol.-Prog. Ser., 357, 291–299, 2008.

Koppelmann, R., Weikert, H., Halsband-Lenk, C., and Jennerjahn, T. C.: Mesozooplankton community respiration and its relation to particle flux in the oligotrophic eastern Mediterranean, Global Biogeochem. Cy., 18, GB1039, doi:10.1029/2003GB002121, 2004.

Lalli, C. M.: Structure and function of the buccal apparatus of *Clione limacina* (Phipps) with a review of feeding in gymnosomatous pteropods, J. Exp. Mar. Biol. Ass. UK, 4, 101–118, 1970.

Lalli, C. M. and Gilmer, R. W.: Pelagic snails: the biology of holoplanktonic gastropod molluscs, Stanford, Stanford University Press, California, 1989.

Larson, R. J.: Water content, organic content, and carbon and nitrogen composition of medusae from the northeast Pacific, J. Exp. Mar. Biol. Ecol., 99, 107–120, doi:10.1016/0022-0981(86)90231-5, 1986.

Leblanc, K., Aristegui, J., Armand, L., Assmy, P., Beker, B., Bode, A., Breton, E., Cornet, V., Gibson, J., Gosselin, M.-P., Kopczynska, E., Marshall, H., Peloquin, J., Piontkovski, S., Poulton, A. J., Queguiner, B., Schiebel, R., Shipe, R., Stefels, J., van Leeuwe, M. A., Varela, M., Widdicombe, C., and Yallop, M.: A global diatom database – abundance, biovolume and biomass in the world ocean, Earth Syst. Sci. Data Discuss., 5, 147–185, doi:10.5194/essdd-5-147-2012, 2012.

Le Quéré, C., Harrison, S. P., Prentice, C., Buitenhuis, E. T., Aumonts, O., Bopp, L., Claustre, H., da Cunha, L. C., Geider, R., Giraud, X., Klaas, C., Kohfeld, K. E., Legendre, L., Manizza, M., Plattss, T., Rivkin, R., Sathyendranath, S., Uitz, J., Watson, A. J., Wolf-Gladrow, D.: Ecosystem dynamics based on plankton functional types for global ocean biochemistry models, Glob. Change Biol., 11, 2016–2040, 2005.

Little, W. S. and Copley, N. J.: WHOI Silhouette DIGITIZER, Version 1.0, Users Guide, WHOI Technical Report, Woods Hole Oceanographic Institution, 2003.

Lochte, K. and Pfannkuche, O.: Processes driven by the small sized organisms at the water-sediment interface, in: Ocean Margin Systems, edited by: Wefer, G., Billet, D., Hebbeln, D., Jørgensen, B. B., Schlüter, M., and Weering, T. C., Springer, Heidelberg, Germany, 2003.

Longhurst, A.: Ecological Geography of the Sea, Academic Press, USA, 2007.

Luo, Y.-W., Doney, S. C., Anderson, L. A., Benavides, M., Bode, A., Bonnet, S., Bostrom, K. H., Bottjer, D., Capone, D. G., Carpenter, E. J., Chen, Y. L., Church, M. J., Dore, J. E., Falcon, L. I., Fernandez, A., Foster, R. A., Furuya, K., Gomez, F., Gundersen, K., Hynes, A. M., Karl, D. M., Kitajima, S., Langlois, R. J., LaRoche, J., Letelier, R. M., Maranon, E., McGillicuddy Jr., D. J., Moisander, P. H., Moore, C. M., Mourino-Carballido, B., Mulholland, M. R., Needoba, J. A., Orcutt, K. M., Poulton, A. J., Raimbault, P., Rees, A. P., Riemann, L., Shiozaki, T., Subramaniam, A., Tyrrell, T., Turk-Kubo, K. A., Varela, M., Villareal, T. A., Webb, E. A., White, A. E., Wu, J., and Zehr, J. P.: Database of diazotrophs in global ocean: abundances, biomass and nitrogen fixation rates, Earth Syst. Sci. Data Discuss., 5, 47–106, doi:10.5194/essdd-5-47-2012, 2012.

Marrari, M., Daly, K. L., Timonin, A., and Semenova, T.: The zooplankton of Marguerite Bay, Western Antarctic Peninsula – Part I: Abundance, distribution, and population response to variability in environmental conditions, Deep-Sea Res. Pt. II, 58, 1599–1613, doi:10.1016/j.dsr2.2010.12.007, 2011.

Mazzocchi, M. G., Christou, E., Rastaman, N., and Siokou-Frangou, I.: Mesozooplankton distribution from Sicily to Cyprus (Eastern Mediterranean): I. General aspects, Oceanol. Acta, 20, 521–535, 1997.

Mileikovsky, S. A.: Breeding and larval distribution of the pteropod *Clione limacina* in the North Atlantic, Subarctic and North Pacific Oceans, Mar. Biol., 6, 317–334, 1970.

Milliman, J. D. and Droxler, A. W.: Neritic and pelagic carbonate sedimentation in the marine environment: Ignorance is not bliss, Geologische Rundschau, 85, 496–504, 1996.

Moraitou-Apostolopoulou, M., Zervoudaki, S., and Kapiris, K.: Mesozooplankton abundance in waters of the Aegean Sea, Hellenic Center of Marine Research, Institut of Oceanography, Hydrodynamics and Biogeochemical Fluxes in the Straits of the Cretan Arc (project), Greece, 2008.

Mousseau, L., Fortier, L., and Legendre, L.: Annual production of fish larvae and their prey in relation to size-fractioned primary production (Scotian Shelf, NW Atlantic), ICES J. Mar. Sci., 55, 44–57, 1998.

Nishikawa, J., Matsuura, H., Castillo, L. V., Wilfredo, L. C., and Nishida, S.: Biomass, vertical distribution and community structure of mesozooplankton in the Sulu Sea and its adjacent waters, Deep-Sea Res. Pt. II, 54, 114–130, doi:10.1016/j.dsr2.2006.09.005, 2007.

NMFS-COPEPOD: The Global Plankton Database, NOAA National Oceanic and Atmospheric Administration, US Department of Commerce (http://www.st.nfms.noaa.gov/plankton), 2011.

Pakhomov, E. A. and Perissinotto, R.: Mesozooplankton community structure and grazing impact in the region of the Subtropical Convergence south of Africa, J. Plankton Res., 19, 675–691, 1997.

Pane, L., Feletti, M., Francomacaro, B., and Mariottini, G. L.: Summer coastal zooplankton biomass and copepod community structure near Italian Terra Nova Base (Terra Nova Bay, Ross Sea, Antarctica), J. Plankton Res., 26, 1479–1488, doi:10.1093/plankt/fbh135, 2004.

Perissinotto, R.: Mesozooplankton size-selectivity and grazing impact on the phytoplankton community of the Prince Edward Archipelago (Southern Ocean), Mar. Ecol.-Prog. Ser., 79, 243–258, 1992.

Ramfos, A., Isari, S., and Rastaman, N.: Mesozooplankton abundance in water of the Ionian Sea (March 2000), Department of Biology, University of Patras, 2008.

Rogachev, K. A., Carmack, E. C., and Foreman, M. G. G.: Bowhead whales feed on plankton concentrated by estuarine and tidal currents in Academy Bay, Sea of Okhotsk, Cont. Shelf Res., 28, 1811–1826, doi:10.1016/j.csr.2008.04.014, 2008.

Schalk, P. H.: Spatial and seasonal variation in pteropods (Mollusca) of Indo-Malayan waters related to watermass distribution, Mar. Biol., 105, 59–71, 1990.

Schiebel, R. and Movellan, A.: First-order estimate of the planktic foraminifer biomass in the modern ocean, Earth Syst. Sci. Data, 4, 75–89, doi:10.5194/essd-4-75-2012, 2012.

Schiebel, R., Waniek, J., Zeltner, A., and Alves, M.: Impact of the Azores Front on the distribution of planktic foraminifers, shelled gastropods, and coccolithophorids, Deep-Sea Res. Pt. II, 49, 4035–4050, 2002.

Schnack-Schiel, S. B. and Cornils, A.: Zooplankton abundance measured on Apstein net samples during cruise CISKA2005,

Alfred Wegener Institute for Polar and Marine Research, Science for the Protection of Indonesian Coastal Environment (project), Bremerhaven, 2009.

Seibel, B. A. and Dierssen, H. M.: Cascading trophic impacts of reduced biomass in the Ross Sea, Antarctica: Just the tip of the iceberg?, Biol. Bull., 205, 93–97, 2003.

Siokou-Frangou, I., Christou, E., and Rastman, N.: Mesozooplankton abundance in waters of the Ionian Sea, Hellenic Center of Marine Research, Institut of Oceanography, Physical Oceanography of the Eastern Mediterranean (project), Greece, 2008.

Solis, N. B. and von Westernhagen, H.: Vertical distribution of Euthecosomatous Pteropods in the Upper 100 m of the Hilutangan Channel, Cebu, The Philippines, Mar. Biol., 48, 79–87, 1978.

Swadling, K. M., Penot, F., Vallet, C., Rouyer, A., Gasparini, S., Mousseau, L., Smith, M., and Goffart, A.: Interannual variability of zooplankton in the Dumont d'Urville sea (139° E–146° E), east Antarctica, 2004–2008, Polar Sci., 5, 118–133, doi:10.1016/j.polar.2011.03.001, 2011.

Tréguer, P., Legendre, L., Rivkin, R. T., Raueneau, O., and Dittert, N.: Water column biogeochemistry below the euphotic zone, Ocean biogeochemistry: The role of the ocean carbon cycle in global change, edited by: Fasham, M. J. R., Global Change – The IGBP Series (closed), 145–156, doi:10.1007/978-3-642-55844-3_7, 2003.

Van der Spoel, S.: Growth, reproduction and vertical migration in *Clio pyramidata* Linne, 1767 forma *lunceolata* (Lesueur, 1813), with notes on some other Cavoliniidae (Mollusca, Pteropoda), Beaufortia, 281, 117–134, 1973.

Volkov, A. F.: Mean Annual Characteristics of Zooplankton in the Sea of Okhotsk, Bering Sea and Northwestern Pacific (Annual and Seasonal Biomass Values and Predominance, ISSN 1063-0740, Russ. J. Mar. Biol., 34, 437–415, doi:10.1134/S106307400807002X, 2008.

Ward, P., Whitehouse, M., Shreeve, R., Thorpe, S., Atkinson, A., Korb, R., Pond, D., and Young, E.: Plankton community structure south and west of South Georgia (Southern Ocean): Links with production and physical forcing, Deep-Sea Res. Pt. I, 54, 1871–1889, doi:10.1016/j.dsr.2007.08.008, 2007.

Wells Jr., F. E.: Effects of Mesh Size on Estimation of Population Densities of Tropical Euthecosomateus Pteropods, Mar. Biol., 20, 347–350, 1973.

Wells Jr., F. E.: Seasonal patterns of abundance and reproduction of euthecosomatous pteropods off Barbados, West Indies, Veliger, 18, 241–248, 1976.

Werner, I.: Living conditions, abundance and biomass of under-ice fauna in the Storfjord area (Western Barents Sea, Arctic) in late winter (March 2003), Polar Biol., 28, 311–318, 2005.

Wormuth, J. H.: Vertical distributions and diel migrations of Euthecosomata in the northwest Sargasso Sea, Deep-Sea Res., 28, 1493–1515, doi:10.1016/0198-0149(81)90094-7, 1981.

Wormuth, J. H.: The role of cold-core Gulf Stream rings in the temporal and spatial patterns of euthecosomatous pteropods, Deep-Sea Res., 32, 773–788, 1985.

Zervoudaki, S., Christou, E., Siokou-Frangou, I., and Zoulias, T.: Mesozooplankton abundance in water of the Aegean Sea, Hellenic Center of Marine Research, Institut of Oceanography, Invest. of new marine biol. resources in deep waters of Ionian and Aegean Seas, Greece, 2008.

ZooDB – Zooplankton database, Plankton sample analysis supported by NSF grants to M. D. Ohman, Scripps Institution of Oceanography and by the SIO Pelagic Invertebrates Collection, http://oceaninformatics.ucsd.edu/zoodb/#, 2011.